GENERALIZED POLYNOMIAL CHAOS AND DISPERSIVE DIELECTRIC MEDIA

ERIN BELA AND ERIK HORTSCH

ADVISOR: PROFESSOR GIBSON
OREGON STATE UNIVERSITY

ABSTRACT. We investigate polynomial chaos as a method to improve the accuracy of the Debye model and allow for easy simulation using the Finite Difference Time Domain (FDTD) method. We develop a framework for incorporating distributions of relaxation times using polynomial chaos and demonstrate that the resultant system adds no physical conditions. We conclude by demonstrating the exponential convergence of the system under a correct choice of polynomials and show how an inverse problem may be formulated to determine parameters of the distribution from experimental data or comparison with another model.

1. INTRODUCTION

Many modern technologies rely on the transmission of electromagnetic pulses. Often these pulses must travel through dispersive dielectric materials. One potential application of these results is the use of ultrawideband(UWB) microwave pulses in cancer detection. Such an approach has the advantages of being able to detect smaller tumors and being less harmful than exposing a patient to X-ray radiation. Also of interest is studying the effects of terahertz radiation, used in airport security screeners, on human tissue.While most of these materials are well understood, there are still some holes in current numerical methods. Of greatest interest is the relaxation times of these media. In past models, relaxation time was often assumed to be constant, however, anomaly dispersive media may be better described using a distribution of relaxation times [4]. For the current work we focus on creating a framework by which simulations can be carried out using a first order ODE model for polarization with different distributions of relaxation times such as uniform, beta, gamma and possibly log-normal. We begin by introducing Maxwell's equations for dispersive media. We then introduce polynomial chaos as a way of including distributions of parameters before finally developing a FDTD method for simulation. We perform a preliminary stability analysis on the resultant system and demonstrate its exponential convergence. Finally, we conclude by formulating an inverse problem , which may then be used obtain a distribution of relaxation times from experimental data.

1.1. Maxwell's Equations.

We begin by introducing Maxwell's equations, which govern the behavior of electromagnetic fields. Our initial goal is to simulate the behavior of such fields in a dispersive dielectric media, namely a Debye media. The following gives the differential form of Maxwell's equations, where **E** and **H** are the electric and magnetic fields, respectively, **D** and **B** are the electric and magnetic flux densities, respectively, and the scalar ρ represents the density of

Date: August 13, 2010.
This work was done during the Summer 2010 REU program in Mathematics at Oregon State University.

free electric charges unaccounted for in the electric polarization. The conduction current density is given by $\mathbf{J}$. Maxwell's equations are

$$\frac{\partial \mathbf{D}}{\partial t} + \mathbf{J} = \nabla \times \mathbf{H} \tag{1}$$

$$\frac{\partial \mathbf{B}}{\partial t} = -\nabla \times \mathbf{E} \tag{2}$$

$$\nabla \cdot \mathbf{D} = \rho \tag{3}$$

$$\nabla \cdot \mathbf{B} = 0. \tag{4}$$

The Constitutive Laws describe the response of the medium to the electromagnetic field

$$\mathbf{D} = \varepsilon_0 \varepsilon_\infty \mathbf{E} + \mathbf{P} \tag{5}$$

$$\mathbf{B} = \mu \mathbf{H} + \mathbf{M} \tag{6}$$

$$\mathbf{J} = \sigma \mathbf{E} + \mathbf{J}_s. \tag{7}$$

In the equations above, $\mathbf{P}$ refers to the macroscopic polarization, $\mathbf{M}$ the magnetization, and $\mathbf{J}_s$ the source current density. The parameters ε_0 and ε_∞ are the permittivity of free space and the relative permittivity, respectively, while μ is the magnetic permeability and σ is the electric conductivity. By combining equations (1), (5) and (7) while neglecting the source term for simplicity we get,

$$\varepsilon_0 \varepsilon_\infty \frac{\partial \mathbf{E}}{\partial t} = -\sigma \mathbf{E} - \frac{\partial \mathbf{P}}{\partial t} + \nabla \times \mathbf{H}. \tag{8}$$

Combining equations (2) and (6) under the assumptions that there is no magnetization and that $\mu = \mu_0$ we get,

$$\mu_0 \frac{\partial \mathbf{H}}{\partial t} = -\nabla \times \mathbf{E}. \tag{9}$$

For the purposes of the simulations to follow we will restrict to one dimension, however, the methods described below apply directly to three dimensions. We assume that all waves travel in the z direction, have an electric field oscillating in the x direction and a magnetic field oscillating in the y direction. Taking this into consideration equations (8) and (9) become,

$$\tilde{\varepsilon}_\infty \frac{\partial E}{\partial t} = -\frac{\partial H}{\partial z} - \sigma E - \frac{\partial P}{\partial t} \tag{10}$$

$$\frac{\partial H}{\partial t} = -\frac{1}{\mu_0} \frac{\partial E}{\partial z} \tag{11}$$

where $\tilde{\varepsilon}_\infty := \varepsilon_\infty \varepsilon_0$, $E := \mathbf{E}_x$, $H := \mathbf{H}_y$, $P := \mathbf{P}_x$.

1.2. **Polarization Models.** For the purposes of this paper we are concerned with the way in which electromagnetic waves propagate through Debye media. These media have a polarization which can be expressed in convolution form as:

$$\mathbf{P}(t,\mathbf{x}) = g \star \mathbf{E}(t,\mathbf{x}) = \int_0^t g(t-s,\mathbf{x};q)\mathbf{E}(s,\mathbf{x})ds \tag{12}$$

where in Debye $q = \{\varepsilon_s, \varepsilon_\infty, \tau\}$. The function g is the dielectric response function (DRF) which can be thought of as representing the memory effect caused by the dielectric. For Debye materials this DRF is,

$$g(t,\mathbf{x}) = \frac{\tilde{\varepsilon}_d}{\tau} e^{-t/\tau} \tag{13}$$

where $\tilde{\varepsilon}_d := \varepsilon_0(\varepsilon_s - \varepsilon_\infty)$ and τ is the relaxation time, which is typically taken to be a scalar. Substituting equation (12) into equation (5) and taking the Laplace transform in time we get,

$$\hat{\mathbf{D}} = \varepsilon(\omega)\hat{\mathbf{E}} \tag{14}$$

where ω is the angular frequency and $\varepsilon(\omega)$ is the complex permittivity. For the Debye model the complex permittivity is given by,

$$\varepsilon(\omega) = \varepsilon_\infty + \frac{\varepsilon_d}{1 - i\omega\tau}. \tag{15}$$

More realistically τ it can be modeled as random variable with a probability distribution. When this is the case we will refer to (15) as the *stochastic complex permittivity*.

1.3. **Distributions.** In previous years, numerical methods to approximate solutions to Maxwell's Equations have relied on the assumption that certain parameters, such as relaxation time, of the medium can be approximated by their mean values. This was later improved upon by assuming uniform distributions of these parameters. This, however, is still inaccurate as relaxation times appear to follow a log-normal distribution [4], which could be approximated more closely by a beta or gamma distribution. In order to incorporate these distributions we must first restate our polarization term to include distributions of τ. Borrowing from Banks and Gibson [2] we define the *stochastic polarization* as,

$$\mathcal{P}(t,z) = \int_{\tau_a}^{\tau_b} \mathrm{P}(t,z;\tau)dF(\tau) \tag{16}$$

where $F(\tau)$ is the density function for τ. This can be expressed as the solution to an ordinary differential equation using τ as a random variable. For the Debye model the *stochastic ordinary differential equation* (SODE) is,

$$\tau\frac{\partial \mathcal{P}}{\partial t} + \mathcal{P} = \tilde{\varepsilon}_d E. \tag{17}$$

The stochastic polarization is the microscopically chaotic polarization that is influenced by distributions of τ. We take the macroscopic polarization, which appears in Maxwell's equations and the constitutive laws to be the expected value of the stochastic polarization.

2. Polynomial Chaos

Generalized polynomial chaos is a method for expressing stochastic solutions in terms of truncated expansions of orthogonal polynomials of the random inputs [18]. Different types of orthogonal polynomials may be chosen to achieve better, sometimes exponential, convergence. First we begin by expressing stochastic polarization at each point in space as an expansion in orthogonal polynomials [11]:

$$\mathcal{P}(\xi) = \sum_{i=0}^{\infty} \alpha_i(t)\phi_i(\xi) \tag{18}$$

where $\phi_i(\xi)$ is the ith orthogonal polynomial spanning our random space and ξ is a random variable with some standard distribution (e.g. U[-1,1]). We may assume that the stochastic relaxation is given by $\tau = r\xi + m$ where $m, r > 0$ Plugging the solution (18) into equation (17) results in,

$$(r\xi + m)\sum_{i=0}^{\infty} \dot{\alpha}_i(t)\phi_i(\xi) + \sum_{i=0}^{\infty} \alpha_i(t)\phi_i(\xi) = \tilde{\varepsilon}_d E \tag{19}$$

where m and r are shift and scaling parameters, respectively.

All orthogonal polynomials have a recurrence relation which can be expressed in the form[18],

$$\xi\phi_n(\xi) = a_n\phi_{n+1}(\xi) + b_n\phi_n(\xi) + c_n\phi_{n-1}(\xi). \tag{20}$$

We substitute (20) into equation (19) in order to remove the explicit dependence on the random variable ξ. This gives

$$r\sum_{i=0}^{\infty} \dot{\alpha}_i(t)\left[a_i\phi_{i+1}(\xi) + b_i\phi_i(\xi) + c_i\phi_{i-1}(\xi)\right] + \sum_{i=0}^{\infty}\left[\alpha_i(t) + m\dot{\alpha}_i(t)\right]\phi_i(\xi) = \tilde{\varepsilon}_d E. \tag{21}$$

Projecting onto the finite dimensional random space spanned by $\{\phi_j\}_{j=0}^{p}$ by taking the weighted inner product with each basis function produces:

$$\begin{aligned} r\sum_{i=0}^{p} \dot{\alpha}_i(t)\left[a_i\langle\phi_{i+1},\phi_j\rangle_w + b_i\langle\phi_i,\phi_j\rangle_w + c_i\langle\phi_{i-1},\phi_j\rangle_w\right] \\ + \sum_{i=0}^{p}\left[\alpha_i(t) + m\dot{\alpha}_i(t)\right]\langle\phi_i,\phi_j\rangle_w = \tilde{\varepsilon}_d E\langle\phi_0,\phi_j\rangle_w. \end{aligned} \tag{22}$$

In the above, $\langle\phi_i,\phi_j\rangle_w$ is the weighted inner product of ϕ_i and ϕ_j and is defined to be:

$$\begin{aligned} \langle\phi_i,\phi_j\rangle_w := &\int_\Omega \phi_i(\xi)\phi_j(\xi)W(\xi)d\xi \\ =&\delta_{ij}\sqrt{h_i h_j} \end{aligned} \tag{23}$$

where δ_{ij} is the Kronecker delta function, $W(\xi)$ is chosen to be the weighting function with respect to which polynomials are orthogonal over the domain Ω, and $h_i := \langle\phi_i,\phi_i\rangle_w$.

This produces a system of equations which can be expressed in matrix form as:

$$\mathrm{A}\vec{\dot{\alpha}}(t) + \vec{\alpha}(t) = \vec{f} \tag{24}$$

where $\mathrm{A} = r\mathrm{M} + m\mathrm{I}$ and

$$\mathrm{M} = \begin{pmatrix} b_0 & c_1 & 0 & \cdots & 0 \\ a_0 & b_1 & c_2 & & \vdots \\ 0 & \ddots & \ddots & \ddots & 0 \\ \vdots & & a_{p-2} & b_{p-1} & c_p \\ 0 & \cdots & 0 & a_{p-1} & b_p \end{pmatrix} \text{ and } \vec{f} = \begin{pmatrix} \tilde{\varepsilon}_d E \\ 0 \\ \vdots \\ 0 \end{pmatrix}$$

where a_i, b_i and c_i are the recursion coefficients. Note that the deterministic value $\vec{f}$ forces the system and is dependent the electric field, which itself depends on the expected value value $\mathrm{P} = \mathbb{E}[\mathcal{P}]$. This can be approximated by α_0 [18]. If the chosen set of orthogonal polynomials are orthogonal with respect to the density function of the random variable ξ then the error in the projection, and in the mean value, converges exponentially with p. We replace the SODE (17) with the deterministic system of ODEs (24).

2.1. **Scaling the polynomials.** In order for the orthogonal polynomials to be applied to a distribution of relaxation times they must be scaled so that they are orthogonal over the correct interval. This can be done linearly and does not affect they recurrence relation. The polynomials may be scaled in this manner so that they are defined over the arbitrary interval from a to b:

$$\phi_n(\xi) = \phi_n\left(2\frac{\tau - a}{b - a} - 1\right) \tag{25}$$

thus

$$\begin{aligned} \xi &= 2\frac{\tau - a}{b - a} - 1 \\ \tau &= \frac{b - a}{2}\xi + \frac{b + a}{2}. \end{aligned} \tag{26}$$

Since $\tau := r\xi + m$

$$r = \frac{b - a}{2} \text{ and } m = \frac{b + a}{2} \tag{27}$$

This is a fairly intuitive result, m is the midpoint between a and b, the center of the distribution, and r is the distance from the midpoint to either edge of the distribution (radius). Note that for many distributions the midpoint is not the mean.

2.2. **Legendre Polynomials.** The Legendre Polynomials are a set of orthogonal polynomials which are orthogonal with respect to a constant over the domain $\Omega = [-1, 1]$. This means that they are ideally suited for characterizing uniformly distributed random variables. The constants for their recurrence relation are [18]:

$$\begin{aligned} a_n &= \frac{n + 1}{2n + 1} \\ b_n &= 0 \\ c_n &= \frac{n}{2n + 1} \end{aligned}$$

It should be noted that the Legendre polynomials are a special case of the Jacobi Polynomials where α and β are zero. The matrix A for the case when $p = 2$ is

$$A = \begin{pmatrix} m & \frac{1}{3}r & 0 \\ r & m & \frac{2}{5}r \\ 0 & \frac{2}{3}r & m \end{pmatrix}.$$

2.3. **Jacobi Polynomials.** The Jacobi Polynomials are orthogonal with respect to the following weighting function [18]:

$$w(\xi) = (\xi - 1)^{\alpha}(1 + \xi)^{\beta}$$

This closely resembles the probability density function of the beta distribution:

$$P(x) = \frac{(1-x)^{\alpha}x^{\beta}}{B(\alpha+1, \beta+1)}.$$

However, in order for us to use these polynomials, both must be scaled so that they are valid over the interval from a to b. This is done by a simple linear substitution and produces:

$$w(\tau) = \left(\frac{2}{b-a}\right)^{\alpha+\beta}(\tau - a)^{\alpha}(\tau - b)^{\beta}$$
$$P(\tau) = \frac{(b-\tau)^{\alpha}(\tau - a)^{\beta}}{B(\alpha+1, \beta+1)(b-a)^{\alpha+\beta}}.$$

We can ignore all of the terms which are constants with respect to τ since they can simply be factored into the h_i term produced when taking the inner product, and this term cancels. Therefore the scaled polynomials are orthogonal with respect to the scaled Beta distribution.

The recurrence relation for Jacobi Polynomials has the following coefficients[18]:

$$\begin{aligned} a_n &= \frac{2(n+1)(n+\alpha+\beta+1)}{(2n+\alpha+\beta+1)(2n+\alpha+\beta+2)} \\ b_n &= \frac{\beta^2 - \alpha^2}{(2n+\alpha+\beta)(2n+\alpha+\beta+2)} \\ c_n &= \frac{2(n+\alpha)(n+\beta)}{(2n+\alpha+\beta)(2n+\alpha+\beta+1)} \end{aligned} \tag{28}$$

This recurrence relation holds true for any linear scaling of the random input parameter. As an example, if we choose $\alpha = 2$, $\beta = 5$, and $p = 2$ we obtain the following system for the stochastic polarization model:

$$A = \begin{pmatrix} \frac{1}{3}r + m & \frac{2}{5}r & 0 \\ \frac{2}{9}r & \frac{7}{33}r + m & \frac{14}{33}r \\ 0 & \frac{18}{55}r & \frac{21}{143}r + m \end{pmatrix}.$$

3. Discretization

Combining (10), (11), and (24) we obtain a model for electromagnetic waves propagating through a dispersive dielectric media, which accounts for a distribution of relaxation times τ. We substitute the expected value of the stochastic polarization, $\mathbb{E}(\mathcal{P}) \approx \alpha_0$, for the macroscopic polarization in P in (10).The polynomial chaos model now has the following form:

$$\begin{aligned} \frac{\partial H}{\partial t} &= -\frac{1}{\mu_0}\frac{\partial E}{\partial z} \\ \tilde{\varepsilon}_\infty \frac{\partial E}{\partial t} &= -\frac{\partial H}{\partial z} - \sigma E - \frac{\partial \alpha_0}{\partial t} \\ A\vec{\alpha} + \vec{\alpha} &= \vec{f}. \end{aligned} \tag{29}$$

We can discretize these equations according to the one-dimensional Yee Scheme[19], adding an additional central difference approximation to the polynomial chaos system. This method uses a staggered grid, with both the electric field, E, and the stochastic polarization, $\vec{\alpha}$, evaluated at half-steps in time and integer steps in space, and the magnetic field, H, evaluated at integer steps in time and half-steps in space. In our discretization, we choose j to represent the spatial step and n to represent the time step.

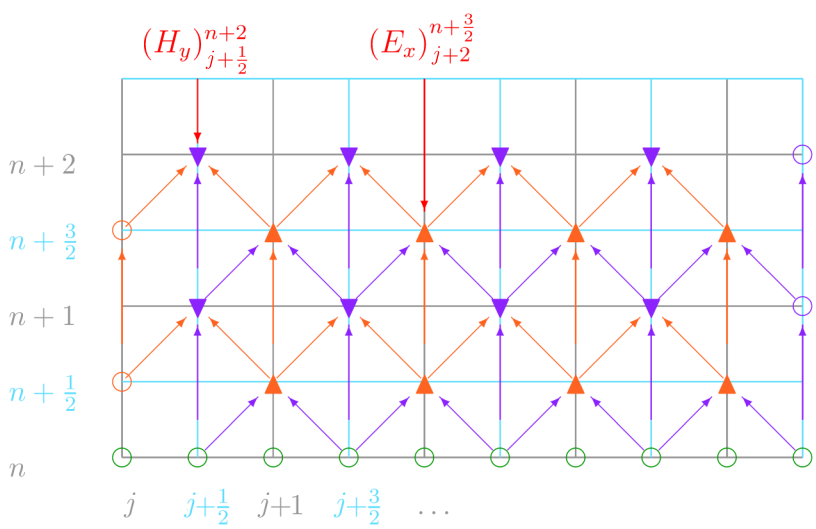

FIGURE 1. Yee Scheme in 1-Dimension

The discretized form of (29) becomes

$$\frac{H^{n+1}_{j+\frac{1}{2}} - H^{n}_{j+\frac{1}{2}}}{\Delta t} = -\frac{1}{\mu_0}\frac{E^{n+\frac{1}{2}}_{j+1} - E^{n+\frac{1}{2}}_{j}}{\Delta z} \tag{30}$$

$$\tilde{\varepsilon}_\infty \frac{E^{n+\frac{1}{2}}_{j} - E^{n-\frac{1}{2}}_{j}}{\Delta t} = -\frac{H^{n}_{j+\frac{1}{2}} - H^{n}_{j-\frac{1}{2}}}{\Delta z} - \sigma\frac{E^{n+\frac{1}{2}}_{j} + E^{n-\frac{1}{2}}_{j}}{2} - \frac{\alpha^{n+\frac{1}{2}}_{0,j} - \alpha^{n-\frac{1}{2}}_{0,j}}{\Delta t} \tag{31}$$

$$\mathrm{A}\frac{\vec{\alpha}_j^{n+\frac{1}{2}}-\vec{\alpha}_j^{n-\frac{1}{2}}}{\Delta t}+\frac{\vec{\alpha}_j^{n+\frac{1}{2}}+\vec{\alpha}_j^{n-\frac{1}{2}}}{2}=\frac{\vec{f}_j^{n+\frac{1}{2}}+\vec{f}_j^{n-\frac{1}{2}}}{2}. \tag{32}$$

Multiplying both sides of the discretized polynomial chaos system (32) by $2\Delta t$ and rearranging the terms, we see that we can write the system as the matrix equation

$$(2\mathrm{A}+\Delta t I)\vec{\alpha}_j^{n+\frac{1}{2}}=(2\mathrm{A}-\Delta t I)\vec{\alpha}_j^{n-\frac{1}{2}}+\Delta t I(\vec{f}_j^{n+\frac{1}{2}}+\vec{f}_j^{n-\frac{1}{2}}). \tag{33}$$

To derive useful update equations which can be used in programming our simulation, we need to solve for $H_{j+\frac{1}{2}}^{n+1}$, $E_j^{n+\frac{1}{2}}$, and $\vec{\alpha}^{n+\frac{1}{2}}$ explicitly in terms of already known values. Since,

$$\vec{f}_j^{n+\frac{1}{2}}=\begin{bmatrix}\tilde{\varepsilon}_d E_j^{n+\frac{1}{2}}\\ 0\\ \vdots\\ 0\end{bmatrix},$$

we see that equations(31) and (33) are coupled. In order to obtain sequential update equations, we solve (31) for $E_j^{n+\frac{1}{2}}$ and substitute this into the polynomial chaos system. Using the simplifications $\theta := 2\tilde{\varepsilon}_\infty+\sigma\Delta t$ and $\theta^* := 2\tilde{\varepsilon}_\infty-\sigma\Delta t$, we obtain,

$$E_j^{n+\frac{1}{2}}=\frac{1}{\theta}[\theta^* E_j^{n-\frac{1}{2}}-\frac{2\Delta t}{\Delta z}(H_{j+\frac{1}{2}}^n-H_{j-\frac{1}{2}}^n)-2(\alpha_{0,j}^{n+\frac{1}{2}}-\alpha_{0,j}^{n-\frac{1}{2}})]. \tag{34}$$

Substituting this result into (33) and collecting all $\alpha_{i,j}^{n+\frac{1}{2}}$ terms on the left-hand side, and all $\alpha_{i,j}^{n-\frac{1}{2}}$ terms on the right-hand side, the first row of (33) becomes

$$\begin{aligned}[2(rb_0+m+\kappa)+\Delta t]\alpha_{0,j}^{n+\frac{1}{2}}+(2rc_1)\alpha_{1,j}^{n+\frac{1}{2}}&=[2(rb_0+m+\kappa)-\Delta t]\alpha_{0,j}^{n-\frac{1}{2}}+(2rc_1)\alpha_{1,j}^{n-\frac{1}{2}}\\&\quad+(\tilde{\varepsilon}_d\Delta t+\kappa\theta^*)E_j^{n-\frac{1}{2}}-\frac{2\kappa\Delta t}{\Delta z}(H_{j+\frac{1}{2}}^n-H_{j-\frac{1}{2}}^n)\end{aligned}$$

where $\kappa := \frac{\tilde{\varepsilon}_d\Delta t}{\theta}$. Borrowing the representation from (33) we can write this system as

$$(2\tilde{\mathrm{A}}+\Delta t I)\vec{\alpha}^{n+\frac{1}{2}}=(2\tilde{\mathrm{A}}-\Delta t I)\vec{\alpha}^{n-\frac{1}{2}}+\tilde{f}^n, \tag{35}$$

where $\tilde{\mathrm{A}}$ is the matrix A with κ added to the (1,1) entry and $\tilde{f}^n$ is the vector,

$$\tilde{f}^n=\begin{bmatrix}(\tilde{\varepsilon}_d\Delta t+\kappa\theta)E_j^{n-\frac{1}{2}}-\frac{2\kappa\Delta t}{\Delta z}(H_{j+\frac{1}{2}}^n-H_{j-\frac{1}{2}}^n)\\ 0\\ \vdots\\ 0\end{bmatrix}.$$

Lastly, the expression for the magnetic field update is given by

$$H_{j+\frac{1}{2}}^{n+1}=-\frac{\Delta t}{\mu_0\Delta z}[E_{j+1}^{n+\frac{1}{2}}-E_j^{n+\frac{1}{2}}]+H_{j+\frac{1}{2}}^n. \tag{36}$$

The final form of our sequential update equations is:

$$
\begin{aligned}
(2\tilde{\mathrm{A}}+\Delta t I)\vec{\alpha}_j^{n+\frac{1}{2}} &= (2\tilde{\mathrm{A}}-\Delta t I)\vec{\alpha}_j^{n-\frac{1}{2}} + \tilde{f}^n \\
E_j^{n+\frac{1}{2}} &= \frac{1}{\theta^+}[\theta^* E_j^{n-\frac{1}{2}} - \frac{2\Delta t}{\Delta z}(H^n_{j+\frac{1}{2}} - H^n_{j-\frac{1}{2}}) - 2(\alpha_{0,j}^{n+\frac{1}{2}} - \alpha_{0,j}^{n-\frac{1}{2}})] \\
H^{n+1}_{j+\frac{1}{2}} &= -\frac{\Delta t}{\mu_0 \Delta z}[E_{j+1}^{n+\frac{1}{2}} - E_j^{n+\frac{1}{2}}] + H^n_{j+\frac{1}{2}}.
\end{aligned}
\tag{37}
$$

3.1. **The Invertibility of A.** In order for our method (37) to have a solution we must be able to invert the matrix $(2\tilde{A}+\Delta t I)$.

Theorem 3.1. *For the Jacobi and Legendre polynomials the matrix* $(2\tilde{\mathrm{A}}+\Delta t I)$ *is invertible if* $m > r$.

Proof. We start by taking the transpose of the matrix, if this matrix is strictly diagonally dominant it must be non-singular and therefor the original matrix must also be invertible. A matrix is strictly diagonally dominant if

$$
|a_{ii}| > \sum_{j\neq i} |a_{ij}| \text{ for all } i. \tag{38}
$$

Since $b_i \geq 0$ for all i then $(2\tilde{A}+\Delta t I)^{\mathrm{T}}$ has all non-negative entries along the main diagonal, we may ignore the absolute value along these entries. The $\Delta t I$ and κ (which was added to the (1,1) number) may also be dropped, as they only add to the main diagonal and we would like to have a solution for arbitrarily small Δt. Therefore, if A^{T} is diagonally dominant then $(2\tilde{A}+\Delta t I)^{\mathrm{T}}$ is also diagonally dominant. This yields the following conditions on A

$$
\begin{aligned}
b_0 r + m &> |a_0| r \\
b_i r + m &> (|c_i| + |a_i|)\, r \quad \text{for } 0 < i < p \\
b_p r + m &> |c_p| r.
\end{aligned}
\tag{39}
$$

Solving for m, these conditions become:

$$
\begin{aligned}
m &> (|a_0| - b_0)\, r \\
m &> (|c_i| + |a_i| - b_i)\, r \quad \text{for } 0 < i < p \\
m &> (|c_p| - b_p)\, r.
\end{aligned}
\tag{40}
$$

Since the middle condition is always increasing for $i > 0$, only the endpoint needs to be checked for the middle conditions. This means that although there are p+1 conditions, at most, only 3 need to be checked. For Legendre and Jacobi polynomials these conditions converge $m > r$ as p goes to infinity. A similar procedure may be applied to ensure stability when working with other polynomials. Table 3.1 demonstrates this convergence for Legendre Polynomials, the same may be shown for Jacobi Polynomials. □

While A may still be non-singular for some values of $r \geq m$, these would imply the possibility of negative relaxation times which is unphysical.

p	largest eigenvalue	$m > max(\lvert c_i\rvert + \lvert a_i\rvert - b_i)r$	$m > (\lvert c_p\rvert - b_p)r$
1	m = 0.577r	$m > r$	$m > \frac{1}{3}r$
2	$m = 0.775r$	$m > r$	$m > \frac{2}{5}r$
4	$m = 0.906r$	$m > r$	$m > \frac{4}{9}r$
8	$m = 0.968r$	$m > r$	$m > \frac{8}{17}r$
16	$m = 0.991r$	$m > r$	$m > \frac{16}{33}r$
32	$m = 0.997r$	$m > r$	$m > \frac{32}{65}r$

TABLE 1. Maximum eigenvalue compared to diagonally dominant conditions for Legendre Polynomials

4. STABILITY ANALYSIS

We wish to determine the stability properties of the above numerical method (37). A finite difference scheme is **stable** if the errors made at each time step of the calculation do not cause the errors to increase without bound as the computations are continued. We also require that our solution be **convergent**. A convergent scheme is one that better approximates Maxwell's equations as the spatial and temporal step sizes are decreased. Finally, a **consistent scheme** is one that differs from the PDE point-wise by factors that go to zero as Δz and Δt go to zero. The following theorem combines the ideas of convergence, consistency, and stability.

Theorem 4.1. (Lax-Richtmyer Equivalence Theorem) [14]
A consistent finite difference scheme for a partial differential equation for which the initial value problem is well-posed is convergent if and only if it is stable.

It is known that the local truncation error (LTE) of the Yee-Scheme in a non-dispersive media is $O(\Delta t^2) + O(\Delta z^2)$[19]. The central difference approximation in the discretization of polarization adds at most $O(\Delta t^2)$ to the LTE. The finite-dimensional projection also contributes to the LTE, however, due to the exponential convergence we may assume, provided p is sufficiently large, that this error is less than $O(\Delta t^2) + O(\Delta z^2)$. Thus we assume the numerical method (37) is consistent and is in fact second order in space and time. Therefore establishing the stability of the numerical method is sufficient to show convergence.

Plane wave solutions of (37) are of the form:

$$\begin{bmatrix} E_j^n \\ H_j^n \\ \alpha_{0,j}^n \\ \vdots \\ \alpha_{p,j}^n \end{bmatrix} = \begin{bmatrix} \tilde{E} \\ \tilde{H} \\ \tilde{\alpha}_0 \\ \vdots \\ \tilde{\alpha}_p \end{bmatrix} \zeta^n \mathrm{e}^{\mathrm{i}kj\Delta z}. \tag{41}$$

Here, $\mathrm{i} = \sqrt{-1}$, $k = \frac{\omega}{c}$ is the wave number, where c is the speed of light and $\omega = 2\pi f$ is the angular frequency, ζ is the complex time eigenvalue, and $\vec{x} = [\tilde{E}, \tilde{H}, \tilde{\alpha}_0, \cdots, \tilde{\alpha}_p]^T$ is the corresponding

eigenvector. In order for our method to be stable we require that $|\zeta| \leq 1$. We proceed by substituting (41) into our discretized update equations (37).

We note that our system $(2\tilde{\mathrm{A}} + \Delta t I)\vec{\alpha}_j^{n+\frac{1}{2}} = (2\tilde{\mathrm{A}} - \Delta t I)\vec{\alpha}_j^{n-\frac{1}{2}} + \tilde{f}^n$ corresponds to the following system of p equations:

for $i = 0$

(42)
$$[2(rb_0 + m + \kappa) + \Delta t]\alpha_{0,j}^{n+\frac{1}{2}} + (2rc_1)\alpha_{1,j}^{n+\frac{1}{2}} = [2(rb_0 + m + \kappa) - \Delta t]\alpha_{0,j}^{n-\frac{1}{2}} + (2rc_1)\alpha_{1,j}^{n-\frac{1}{2}} + (\tilde{\varepsilon}_d \Delta t + \kappa\theta^*)E_j^{n-\frac{1}{2}} - 2\kappa\frac{\Delta t}{\Delta z}(H_{j+\frac{1}{2}}^n - H_{j-\frac{1}{2}}^n),$$

for $0 < i < p$

(43)
$$(2ra_{i-1})\alpha_{i-1,j}^{n+\frac{1}{2}} + [2(rb_i + m) + \Delta t]\alpha_{i,j}^{n+\frac{1}{2}} + (2rc_{i+1})\alpha_{i+1,j}^{n+\frac{1}{2}} = (2ra_{i-1})\alpha_{i-1,j}^{n-\frac{1}{2}} + [2(rb_i + m) - \Delta t]\alpha_{i,j}^{n-\frac{1}{2}} + (2rc_{i+1})\alpha_{i+1,j}^{n-\frac{1}{2}},$$

and for $i = p$

(44)
$$(2ra_{p-1})\alpha_{p-1,j}^{n+\frac{1}{2}} + [2(rb_p + m) + \Delta t]\alpha_{p,j}^{n+\frac{1}{2}} = (2ra_{p-1})\alpha_{p-1,j}^{n-\frac{1}{2}} + [2(rb_p + m) - \Delta t]\alpha_{p,j}^{n-\frac{1}{2}}.$$

We substitute each component of (41) into the first equation and cancel $\zeta^{n-\frac{1}{2}}\mathrm{e}^{\mathrm{i}kj\Delta z}$ from both sides to obtain

$$[2(rb_0 + m + \kappa) + \Delta t]\zeta\tilde{\alpha}_0 + (2rc_1)\zeta\tilde{\alpha}_1 = [2(rb_0 + m + \kappa) - \Delta t]\tilde{\alpha}_0 + (2rc_1)\tilde{\alpha}_1 + (\tilde{\varepsilon}_d \Delta t + \kappa\theta^*)\tilde{E} - \frac{2\kappa\Delta t}{\Delta z}\zeta^{\frac{1}{2}}(\mathrm{e}^{\frac{\mathrm{i}k\Delta z}{2}} - \mathrm{e}^{-\frac{\mathrm{i}k\Delta z}{2}})\tilde{H}.$$

Using Euler's formula, $\mathrm{e}^{\mathrm{i}\theta} = \cos\theta + \mathrm{i}\sin\theta$, it follows that $\mathrm{e}^{\frac{\mathrm{i}k\Delta z}{2}} - \mathrm{e}^{-\frac{\mathrm{i}k\Delta z}{2}} = 2\mathrm{i}\sin(\frac{k\Delta z}{2})$. Substituting in this identity and simplifying further results in the following equation:

(45)
$$[2\kappa(\zeta - 1) + (2rb_0 + 2m + \Delta t)\zeta - (2rb_0 + 2m - \Delta t)]\tilde{\alpha}_0 + (2rc_1)(\zeta - 1)\tilde{\alpha}_1 - (\tilde{\varepsilon}_d \Delta t + \kappa\theta^*)\tilde{E} + \frac{4\mathrm{i}\kappa\Delta t}{\Delta z}\zeta^{\frac{1}{2}}\sin(\frac{k\Delta z}{2})\tilde{H} = 0.$$

The remaining equations can be derived in a similar fashion and end up being considerably simpler. For our polynomial chaos system, we obtain the following equations:
for $0 < i < p$

$$(2ra_{i-1})(\zeta - 1)\tilde{\alpha}_{i-1} + [(2rb_i + 2m + \Delta t)\zeta - (2rb_i + 2m - \Delta t)]\tilde{\alpha}_i + (2rc_{i+1})(\zeta - 1)\tilde{\alpha}_{i+1} = 0,$$

and for $i = p$

$$(2ra_{p-1})(\zeta - 1)\tilde{\alpha}_{p-1} + [(2rb_p + 2m + \Delta t)\zeta - (2rb_p + 2m - \Delta t)]\tilde{\alpha}_p = 0.$$

Applying the same approach, we obtain the following for the electric and magnetic field updates,

$$(\theta\zeta-\theta^*)\tilde{E}+\frac{4\mathrm{i}\Delta t}{\Delta z}\zeta^{\frac{1}{2}}\sin(\frac{k\Delta z}{2})\tilde{H}+2(\zeta-1)\tilde{\alpha}_0=0. \tag{46}$$

$$(\zeta-1)\tilde{H}+\frac{2\mathrm{i}\Delta t}{\mu_0\Delta z}\zeta^{\frac{1}{2}}\sin(\frac{k\Delta z}{2})\tilde{E}=0 \tag{47}$$

We can write our system as $\mathrm{S}\vec{x}=0$, where $\vec{x}=[\tilde{E},\tilde{H},\tilde{\alpha}_0,\cdots,\tilde{\alpha}_p]^T$,

$$\mathrm{S}=\left[\begin{array}{ccc|c} \theta\zeta-\theta* & \frac{4\mathrm{i}\rho}{c_\infty}\zeta^{\frac{1}{2}} & 2(\zeta-1) & \\ \frac{2\mathrm{i}\rho}{\mu_0 c_\infty}\zeta^{\frac{1}{2}} & \zeta-1 & 0 & 0 \\ -(\tilde{\varepsilon}_d\Delta t+\kappa\theta^*) & \frac{4\mathrm{i}\kappa\rho}{c_\infty}\zeta^{\frac{1}{2}} & 2\kappa(\zeta-1) & \\ \hline & 0 & & 0 \end{array}\right]+\left[\begin{array}{cc|c} 0 & 0 & \\ 0 & 0 & 0 \\ \hline 0 & & (2A+\Delta tI)\zeta-(2A-\Delta tI) \end{array}\right]$$

$\nu:=\frac{c_\infty\Delta t}{\Delta z}$, $c_\infty:=\frac{1}{\sqrt{\mu_0\tilde{\varepsilon}_\infty}}$, and $\rho:=\nu\sin(\frac{k\Delta z}{2})$.

This system has a non-trivial solution if and only if $\det\mathrm{B}=0$. We obtain a characteristic polynomial is of the form

$$\sum_{k=0}^{p+3}q_k\zeta^{p-k}=0$$

4.1. **The Characteristic Polynomial when p=1.** Neglecting conductivity (letting $\sigma=0$), we obtain a polynomial of the following form for $p=1$:

$$q_0\zeta^4+q_1\zeta^3+q_2\zeta^2+q_3\zeta+q_4=0, \tag{48}$$

with coefficients

$$\begin{aligned} q_0&=4|\mathrm{A}|+[(rb_0+m)+\varepsilon_q(rb_1+m)]\Delta t+\varepsilon_q\Delta t^2\\ q_1&=4\rho^2\Delta t^2+2\Delta t[4\mathbf{tr}(\mathrm{A})\rho^2-(rb_0+m)-\varepsilon_q(rb_1+m)]-16|\mathrm{A}|(1-\rho^2)\\ q_2&=2\Delta t^2(4\rho^2-\varepsilon_q)-8|\mathrm{A}|(4\rho^2-3)\\ q_3&=4\rho^2\Delta t^2-2\Delta t[4\mathbf{tr}(\mathrm{A})\rho^2-(rb_0+m)-\varepsilon_q(rb_1+m)]-16|\mathrm{A}|(1-\rho^2)\\ q_4&=4|\mathrm{A}|-[(rb_0+m)+\varepsilon_q(rb_1+m)]\Delta t+\varepsilon_q\Delta t^2. \end{aligned} \tag{49}$$

Note that this is valid for any choice of polynomials. For Jacobi Polynomials, which correspond to a beta distribution of relaxation times we have

$$\begin{aligned} |\mathrm{A}|&=m^2+\frac{2(\beta-\alpha)}{\alpha+\beta+4}rm+\left[\frac{(\beta-\alpha)^2}{(\alpha+\beta+3)(\alpha+\beta+4)}-\frac{1}{\alpha+\beta+3}\right]m^2\\ \mathbf{tr}(\mathrm{A})&=2m+\frac{2(\beta-\alpha)}{\alpha+\beta+4}r, \end{aligned}$$

where b_0 and b_1 defined as in (28). If we let $\alpha = 2$ and $\beta = 5$ the above expressions simplify to

$$|\mathrm{A}| = m^2 + \frac{6}{11}rm - \frac{1}{55}m^2$$
$$\mathbf{tr}(\mathrm{A}) = 2m - \frac{6}{11}r.$$

We also note $b_0 = \frac{1}{3}$ and $b_1 = \frac{7}{33}$. Finally, for Legendre polynomials these coefficients become

$$\begin{aligned}
q_0 &= 4(m^2 - \frac{1}{3}r^2) + 2m\Delta t(\varepsilon_q + 1) + \varepsilon_q \Delta t^2 \\
q_1 &= 16(m^2 - \frac{1}{3}r^2)(\rho^2 - 1) + 4m\Delta t\left[4\rho^2 - \varepsilon_q - 1\right] + 4\rho^2\Delta t^2 \\
q_2 &= 2\Delta t^2(4\rho^2 - \varepsilon_q) - 8(m^2 - \frac{1}{3}r^2)(4\rho^2 - 3) \\
q_3 &= 16(m^2 - \frac{1}{3}r^2)(\rho^2 - 1) - 4m\Delta t\left[4\rho^2 - \varepsilon_q - 1\right] + 4\rho^2\Delta t^2 \\
q_4 &= 4(m^2 - \frac{1}{3}r^2) - 2m\Delta t(\varepsilon_q + 1) + \varepsilon_q \Delta t^2.
\end{aligned} \tag{50}$$

4.2. **Routh-Hurwitz Stability Criterion.** The Routh-Hurwitz Criterion [12] establishes that the polynomial,

$$f(z) = \sum_{k=0}^{N} b_k z^{N-k}, \quad b_0 > 0$$

where b_k are arbitrary constant real coefficients, has no roots in the right-half of the complex-plane only if all the entries of the first column of the Routh Table are non-negative. We construct the Routh Table as follows. The coefficients b_k are arranged in two rows, noting that the leading coefficient always appears in the upper left corner:

$$c_{1,k} = b_{2k}, \text{ for } k = 0, \ldots, \lfloor \frac{N}{2} \rfloor$$
$$c_{2,k} = b_{2k+1}, \text{ for } k = 0, \ldots, \lfloor \frac{N-1}{2} \rfloor$$

The remaining entries in the the table are obtained using the formula:

$$c_{j,k} = -\frac{1}{c_{j-1,0}} \begin{vmatrix} c_{j-2,0} & c_{j-2,k+1} \\ c_{j-1,0} & c_{j-1,k+1} \end{vmatrix}$$

For example, the Routh Table for $f(z) = b_0 z^3 + b_1 z^2 + b_2 z + b_3$ is

b_0	b_2
b_1	b_3
$b^\star$	0
b_4	0

and the Routh Table for $f(z) = b_0 z^4 + b_1 z^3 + b_2 z^2 + b_3 z + b_4$ is,

b_0	b_2	b_4
b_1	b_3	0
$b^\star$	b_4	0
$b^{\star\star}$	0	0
b_4	0	0

where $b^\star = \frac{b_1 b_2 - b_0 b_3}{b_1}$ and $b^{\star\star} = \frac{b^\star b_3 - b_1 b_4}{b^\star}$. We note there is also a special case where we can still have roots in the right-half plane even if all of the entries in the first column of the Routh table are nonnegative. This occurs only when there is a row of zeros in our Routh table.

We can use the Routh-Hurwitz criterion to determine if any of the roots of our stability polynomial lie outside of the unit circle. The transformation

$$\zeta = \frac{z+1}{z-1} \tag{51}$$

maps the outside of the unit circle to the right half plane. Thus if we apply (51) to our characteristic polynomial, $f(\zeta)$, and the resulting polynomial $f(z)$ has no roots in the right-half plane, we can conclude that $f(\zeta)$ has no roots outside of the unit circle and our solution is stable. We consider the stability of our polynomial chaos scheme using Legendre polynomials. We start by considering the case $p = 1$, as the $p = 0$ case corresponds to the traditional single-pole Debye and is outlined by Pereda. [12] The following theorem gives the exact conditions under which our method is stable in this case.

Theorem 4.2. *The numerical polynomial chaos scheme* (37) *is stable for Legendre polynomials with* $p = 1$ *if and only if the following conditions hold*

$$\begin{aligned} m &\geq 0 \\ \nu &\leq 1 \\ \varepsilon_s &\geq \varepsilon_\infty. \end{aligned}$$

Proof. Let $p = 1$ and suppose we choose to use Legendre polynomials in our polynomial chaos system. The characteristic polynomial of the form given in (48) with coefficients given by (50). If we let $\zeta = \frac{z+1}{z-1}$ and simplify by multiplying through by a factor of $\frac{(z-1)^4}{2^4}$ we obtain the polynomial

$$\hat{q}_0 z^4 + \hat{q}_1 z^3 + \hat{q}_2 z^2 + \hat{q}_3 z + \hat{q}_4 = 0, \tag{52}$$

where

$$\begin{aligned} \hat{q}_0 &= \rho^2 \Delta t^2 \\ \hat{q}_1 &= 4m\rho^2 \Delta t \\ \hat{q}_2 &= 4|\mathrm{A}|\rho^2 + (\varepsilon_q - \rho^2)\Delta t^2 \\ \hat{q}_3 &= 2m\Delta t(\varepsilon_q + 1 - 2\rho^2) \\ \hat{q}_4 &= 4|\mathrm{A}|(1 - \rho^2) \end{aligned}$$

$\rho = \nu \sin(\frac{k\Delta z}{2})$ and $\varepsilon_q = \frac{\varepsilon_s}{\varepsilon_\infty}$, and $|A| = m^2 - \frac{1}{3}r^2$. The Routh Table is therefore

$\hat{q}_0$	$\hat{q}_2$	$\hat{q}_4$
$\hat{q}_1$	$\hat{q}_3$	0
$q^\star = \frac{\hat{q}_1\hat{q}_2 - \hat{q}_0\hat{q}_3}{\hat{q}_1}$	$\hat{q}_4$	0
$q^{\star\star} = \frac{q^\star\hat{q}_3 - \hat{q}_1\hat{q}_4}{q^\star}$	0	0
$\hat{q}_4$	0	0

We need the entires in the first column to be nonnegative. We note that $\hat{q}_0$ is always nonnegative. Requiring $\hat{q}_1$ to be nonnegative leads to the stability condition $m \geq 0$. Using our condition for the invertibility of A, $m \geq r$, we see

$$|\mathrm{A}| = m^2 - \frac{1}{3}r^2 \geq \frac{2}{3}m^2 \geq 0$$

Since $|\mathrm{A}|$ is positive we can conclude $\hat{q}_4$ is positive provided $\rho^2 = \nu^2 \sin^2(\frac{k\Delta z}{2}) \leq 1$. Using the worst case, $\sin^2(\frac{k\Delta z}{2}) = 1$, we obtain the C.F.L condition $\nu \leq 1$. Computing $q^\star$ we obtain:

$$q^\star = 4|\mathrm{A}|\rho^2 + \frac{1}{2}(\varepsilon_q - 1)\Delta t^2$$

We note that $0 \leq 4|\mathrm{A}|\rho^2 \leq 4m^2$. Thus $\frac{1}{2}(\varepsilon_q - 1)(\Delta t)^2$ is a lower bound for $q^\star$. Requiring $(\varepsilon_q - 1)(\Delta t)^2$ to be positive will thus insure that $q^\star$ is positive. This leads to the condition

$$\begin{aligned} &\varepsilon_q - 1 \geq 0 \\ &\Rightarrow \varepsilon_q \geq 1 \\ &\Rightarrow \varepsilon_s \geq \varepsilon_\infty \end{aligned}$$

since $\varepsilon_q := \frac{\varepsilon_s}{\varepsilon_\infty}$. We notice that $q^{\star\star}$ will be positive if and only if its numerator is positive (since $q^\star$ must be positive). Computing the numerator we obtain:

$$q^\star\hat{q}_3 - \hat{q}_1\hat{q}_4 = m\Delta t(\varepsilon_q - 1)[(\varepsilon_q + 1 - 2\rho^2)\Delta t^2 + 8|\mathrm{A}|\rho^2]$$

since $m\Delta t(\varepsilon_q - 1)$ is positive given the conditions above, we only need to verify that the term in square brackets is positive. However,

$$\begin{aligned} (\varepsilon_q + 1 - 2\rho^2)\Delta t^2 + 8|\mathrm{A}|\rho^2 &\geq (2 - 2\rho^2)\Delta t^2 + 8|\mathrm{A}|\rho^2 \quad \text{since } \varepsilon_q \geq 1 \\ &= 2(1 - \rho^2)\Delta t^2 + 8|\mathrm{A}|\rho^2 \end{aligned}$$

Since $0 \leq \rho^2 \leq 1, |\mathrm{A}| = m^2 - \frac{1}{3}r^2 \geq 0$, and the sum of two nonnegative terms is nonnegative we can conclude that $q^{\star\star} \geq 0$. Therefore we have shown that the entries in the first column of the Routh Table are nonnegative if and only if $m \geq 0, \nu \leq 1$, and $\varepsilon_s \geq \varepsilon_\infty$. Furthermore these conditions are sufficient to establish the stability of out method in the case $p = 1$. □

This approach can be used to establish the stability of the polynomial chaos model with other choices of orthogonal polynomials as well as for larger values of p. It is worth noting that the only distinction between these results and that of the analysis of the single-pole Debye is the replacement of the condition $\bar{\tau} \geq 0$ by $m \geq 0$. We defined m to be the midpoint of the distribution of relaxation times, while $\bar{\tau}$ in the Debye model analyzed by Pereda is the average relaxation time.

In the case of Legendre chaos, which corresponds to a uniform distribution of τ, the mean and midpoint are the same, but for many other distributions (including beta distributions in general) this is not the case.

Additionally, suppose our distribution is defined on the interval $[a,b]$. Without loss of generality we can assume $a < b$ or $a = b$. The second case we wish to avoid since this represents a delta distribution of τ, which would imply that τ has only a single value, the solution to which is well understood. In addition, empirical data shows that materials such as dry skin represent a wide range of relaxation times, so this is not realistic as well. SInce $r = \frac{b-a}{2}$, it follows r must be nonnegative. Combining this with the invertibility condition we require $0 < r < m$ for our polynomial chaos model.

4.3. **Numerical Stability Analysis.** We use MAPLE to plot the maximum roots of our characteristic polynomial (for the p=1 case) as a function of $k\Delta z$ for $0 \leq k\Delta z \leq \pi$. We begin by considering a uniform distribution of relaxation times from $\frac{\overline{\tau}}{2}$ to $\frac{3\overline{\tau}}{2}$ taking $\overline{\tau} = 8.13 \times 10^{-12}$ seconds as done by Petropoulos [13]. From this we see $m = \overline{\tau}$ and $r = \frac{\overline{\tau}}{2}$. Additional parameters are $\varepsilon_s = 78.2$, $\varepsilon_\infty = 1$, and $\sigma = 5 \times 10^{-4}$. We first consider the case $\nu = 1$ for three temporal different resolutions: $h = 0.1$, $h = 0.01$, and $h = 0.001$, where $h := \frac{\Delta t}{\overline{\tau}}$. These correspond to 10, 100, and 1000 time-steps per mean relaxation time $\overline{\tau}$ respectively. It is evident from the plot that the maximum value of $|\zeta|$ is always less than or equal to 1, which numerically verifies the stability of our method proved in the preceding section.

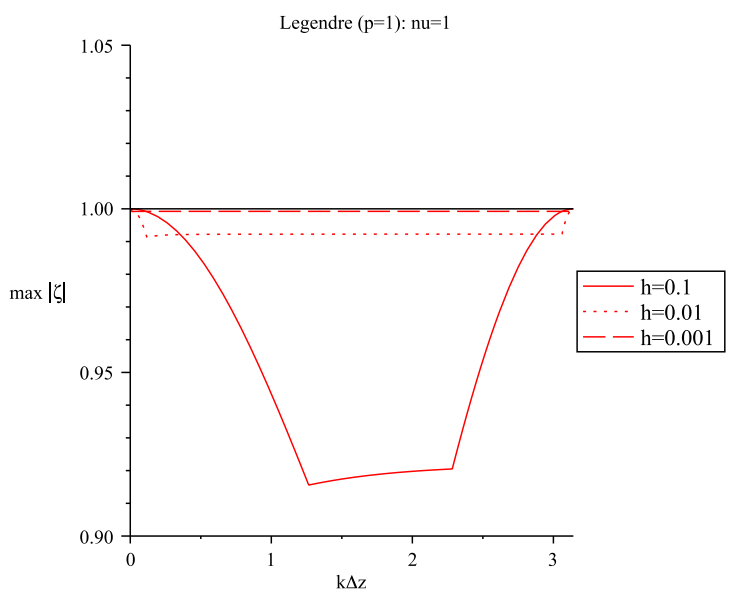

FIGURE 2. The maximum eigenvalue at three different temporal resolutions for the Polynomial Chaos finite-difference scheme as a function of $k\Delta z$ using Legendre Polynomials with $p = 1$ and $\nu = 1$.

We provide as comparison a plot of the maximum eigenvalues for $h = 0.1$ and $\nu = 0.5, 0.75$, and 1. Since $\nu := \frac{c_\infty \Delta t}{\Delta z}$ and $\Delta t = h\overline{\tau}$ it follows that $\Delta z = \frac{c_\infty h\overline{\tau}}{\nu}$. If we fix h and increase the value of ν we

are therefore decreasing the spatial step size.The plot of $\nu = 0.5$ is of particular interest to us as it is the value utilized in our simulation. Once again we see that the method is stable for all of these choices of ν.

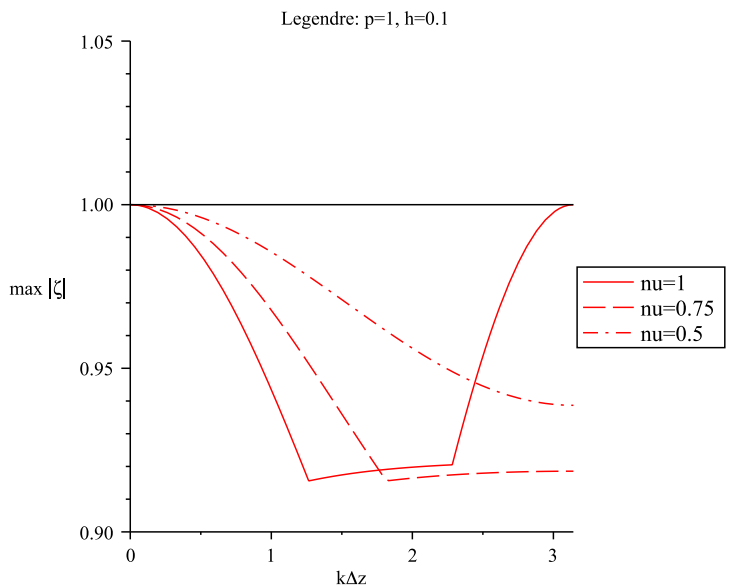

FIGURE 3. The maximum eigenvalue at three different spatial resolutions for the Polynomial Chaos finite-difference scheme as a function of $k\Delta z$ using Legendre Polynomials with $p = 1$ and $h = 0.1$.

For values of $\nu \geq 1$ our method becomes unstable. We consider the plot of $\nu = 1.1$ at three resolutions, $h = 0.1$, $h = 0.01$, and $h = 0.001$. As we can see, this is a rather tight bound, as the the maximum roots now far exceed 1 on the right side of the plot.

Finally we compare the roots of largest magnitude, $max|\zeta|$ for the cases $p = 1$, through $p = 5$. Note that in practice a value of $p = 2$ or $p = 3$ is probably sufficient. We will show in a subsequent section that due to computational limitations the accuracy does not actually improve beyond $p = 6$.

As a comparison we replicate our plots for Jacobi polynomials choosing $\alpha = 2$ and $\beta = 5$. Once again we let $m = \overline{\tau}$ and $r = \frac{\overline{\tau}}{2}$. Note that we have arbitrarily picked these values as they do not necessarily correspond to a distribution of relaxation times in a material of interest. Using the same material parameters, we obtain the following plots. It is of interest to note that there is minimal difference between the plots for Legendre polynomials (Jacobi polynomials with $\alpha = \beta = 0$) and the Jacobi polynomials with $\alpha = 2$ and $\beta = 5$. This is important, as it suggests that the choice of beta distribution itself, provided we have $0 < r < m$, does not change the stability of the polynomial chaos scheme.

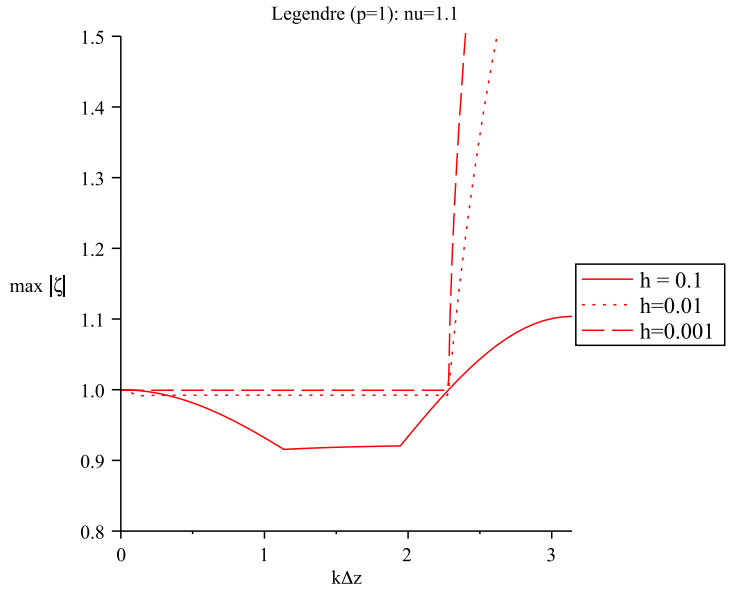

FIGURE 4. The maximum eigenvalue at three different temporal resolutions for the Polynomial Chaos finite difference scheme as a function of $k\Delta z$ using Legendre Polynomials with $p = 1$ and $\nu = 1.1$. This violates our CFL condition of $\nu \leq 1$ and gives an example of an unstable solution since $max|\zeta|$ exceeds 1.

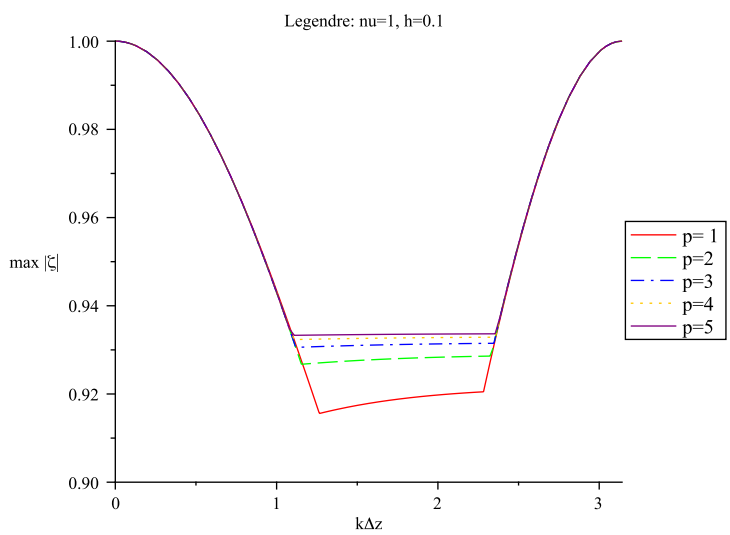

FIGURE 5. The maximum eigenvalue for the Polynomial Chaos finite-difference scheme as a function of $k\Delta z$ using Legendre Polynomials with $\nu = 1$ and $h = 0.1$. The first five values of p are shown.

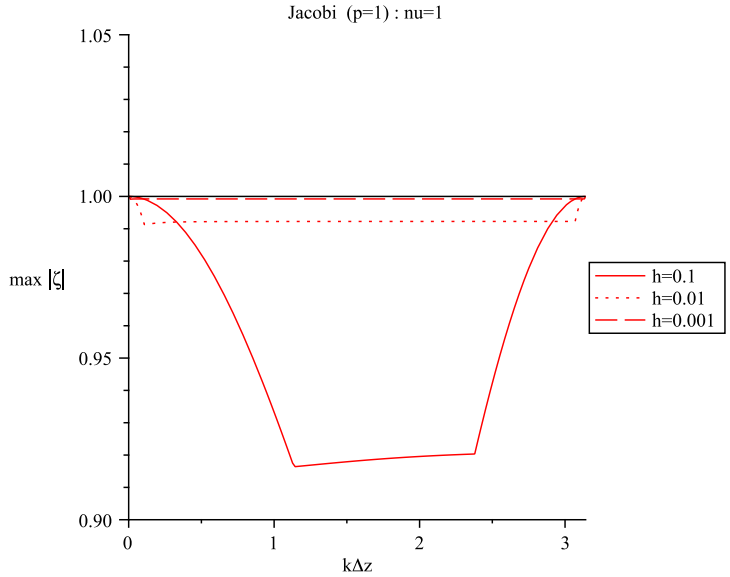

FIGURE 6. The maximum eigenvalue at three different temporal resolutions for the Polynomial Chaos finite-difference scheme as a function of $k\Delta z$ using Jacobi Polynomials ($\alpha = 2$, $\beta = 5$) with $p = 1$ and $\nu = 1$.

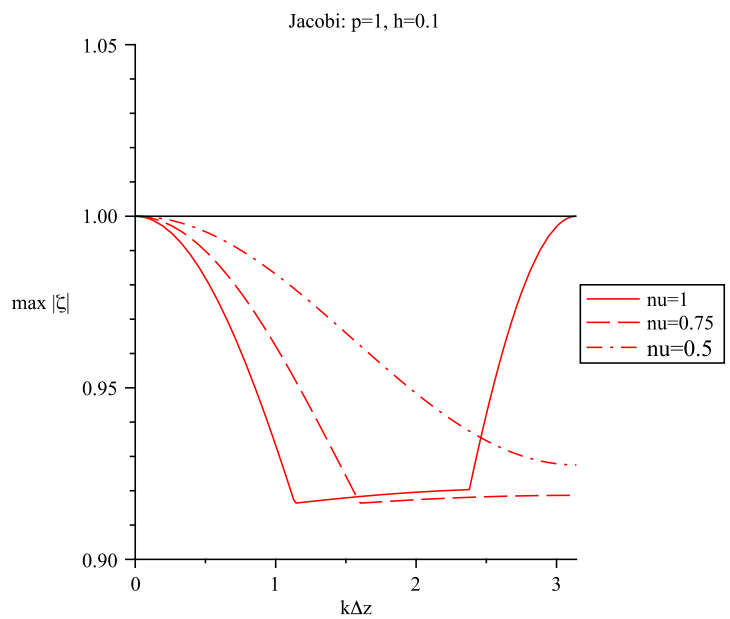

FIGURE 7. The maximum eigenvalue at three different spatial resolutions for the Polynomial Chaos finite-difference scheme as a function of $k\Delta z$ using Jacobi Polynomials($\alpha = 2$, $\beta = 5$) with $p = 1$ and $h = 0.1$.

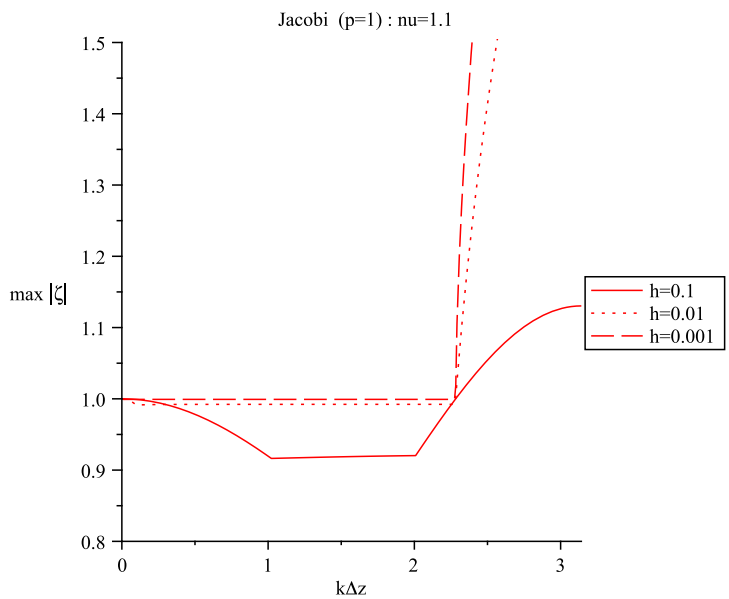

FIGURE 8. The maximum eigenvalue at three different temporal resolutions for the Polynomial Chaos finite difference scheme as a function of $k\Delta z$ using Jacobi Polynomials ($\alpha = 2$, $\beta = 5$) with $p = 1$ and $\nu = 1.1$. This violates our CFL condition of $\nu \leq 1$ and gives an example of an unstable solution since $max|\zeta|$ exceeds 1.

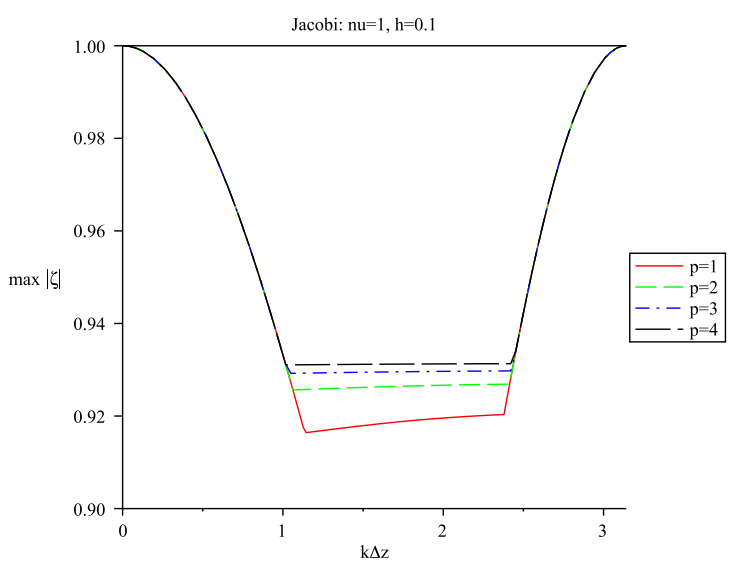

FIGURE 9. The maximum eigenvalue for the Polynomial Chaos finite-difference scheme as a function of $k\Delta z$ using Jacobi Polynomials ($\alpha = 2$, $\beta = 5$) with $\nu = 1$ and $h = 0.1$. The first four values of p are shown.

5. Simulation

To simplify we allowed τ to be uniformly distributed from $\frac{1}{2}\overline{\tau}$ to $\frac{3}{2}\overline{\tau}$ for the purpose of our simulations. The following values were also used in the simulation unless otherwise noted,

Physical Constants:

$$\varepsilon_0 = 8.85419 \times 10^{-12}$$
$$\mu_0 = 4\pi \times 10^{-7}$$
$$c = 3 \times 10^8 = \frac{1}{\sqrt{\mu_0 \varepsilon_0}} \text{ (the speed of light in a vacuum)}$$

Material Parameters:

$$\varepsilon_s = 80.35$$
$$\varepsilon_\infty = 1$$
$$\overline{\tau} = 8.13 \times 10^{-12}$$
$$r = \frac{1}{2}\overline{\tau}$$
$$m = \overline{\tau}$$
$$\sigma = 0$$

Simulation Parameters:

$$f = 10\,\mathbf{GHz} \text{ (the frequency of the simulated pulse)}$$
$$h = 0.01$$
$$\nu = 0.5 \text{ (the CFL condition)}$$
$$\Delta t = h \times \overline{\tau} \text{ (the time step)}$$
$$\Delta z = \frac{c\Delta t}{\nu} \text{ (the spacial step)}$$

5.1. **Convergence.** In order for this method to be useful it must converge to an accurate solution for small values of p. In other words, our method will only be useful if we have to solve a system of only a few equations instead of hundreds. Fortunately this is the case, our method displays exponential convergence and can arrive at a solution accurate to approximately 10^{-12} using only p = 6 and $m = \frac{1}{2}s$ with 16 digits of precision, which corresponds to a seven equation system. It should also be noted that the accuracy can go beyond 10^{-12} for larger value of p, but this would also necessitate more than 16 digits of precision. It should also be noted that changing r affects the rate of convergence, with values closer to 0 causing more rapid convergence, and values closer to m resulting in slower convergence.

The error displayed in Figure 10 is calculated by running a simulation for 0.75×10^{-9} seconds for various values of p ranging from 0 to 12. Then we assume that the result calculated when p is 12 is the most accurate and subtract that data from the results for the other simulations. This gives us a rough estimate of how quickly the method converges. To plot these results we take the absolute value and add machine epsilon $\left(22^{-52} \approx 2.22 \times 10^{-16}\right)$ so that the results display properly on a

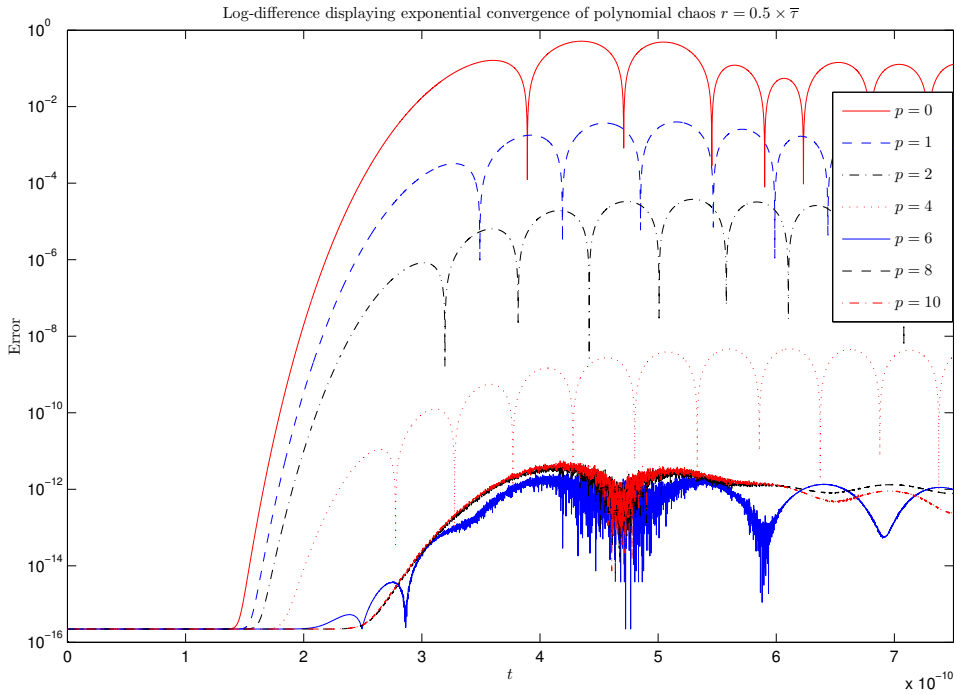

FIGURE 10. Error Calculated for various values of p. $r = \frac{1}{2}\tau$ and $m = \tau$.

log-scale graph. Since this graph can be difficult to read, we also take the maximum value for each value of p and graph that as Figure 11.

When compared with the same data for different values of r this also shows how increasing r leads to slower convergence. The plot for $r = 0$ is not displayed here since it is 0 always. This is because in case when $r = 0$ our matrix which corresponds to our system of equations, becomes a scalar multiple of the identity matrix. Therefore the solution does not change for α_0 as p increases, and the remaining α_i terms are zero.

Changing other parameters also affects the convergence of the method. Since this method is based on FDTD it should converge to an exact solution as Δt goes to 0. In order to demonstrate this we first define the value of Δt as

$$\Delta t := h\overline{\tau}. \tag{53}$$

We will modify the value of Δt by changing our parameter value of h. As Figure 12 shows, our method converges as h and thus Δt tend to 0. Counter intuitively, although our method converges to a more accurate solution as h goes to 0, the noise floor of our method actually rises as displayed in Figure 13. The reason for this increased noise could be any number of things. However, current assumption is that the increased number of time steps could be increasing the number of Local Truncation Errors faster than these errors tend to zero. This implies that there is a sweet spot for Δt, values above or below that would actually decrease the precision of the method.

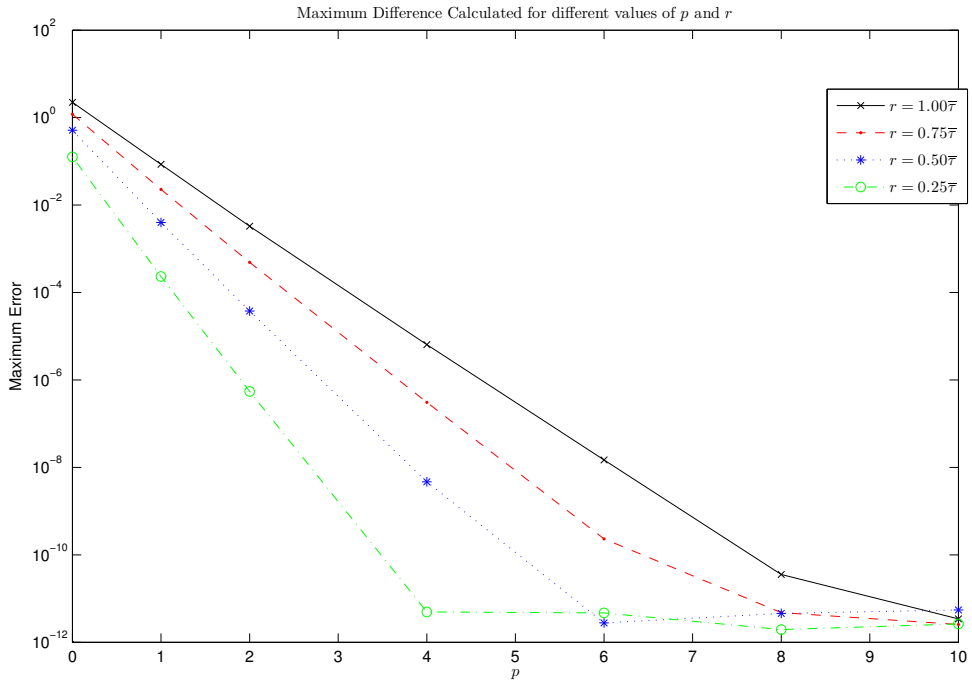

FIGURE 11. Maximum Error for various values of p and r.

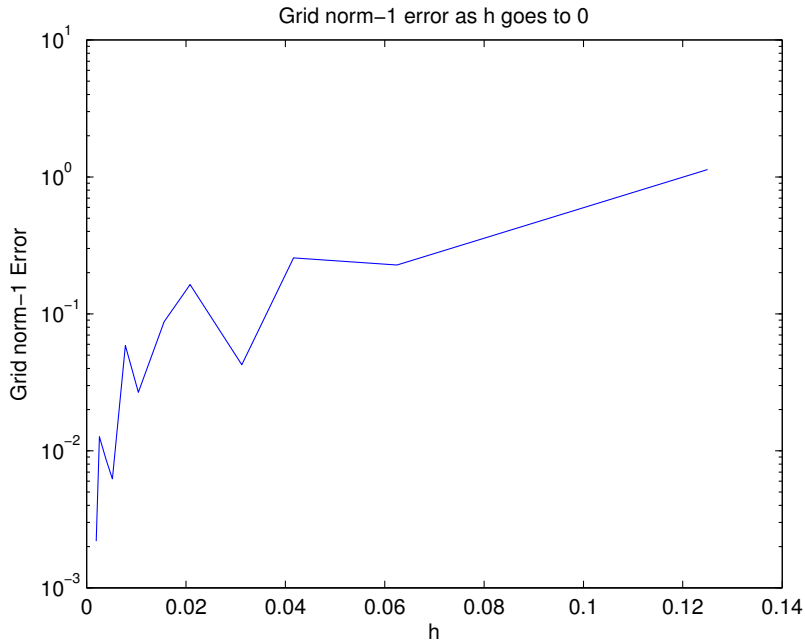

FIGURE 12. The average error for different values of Δt

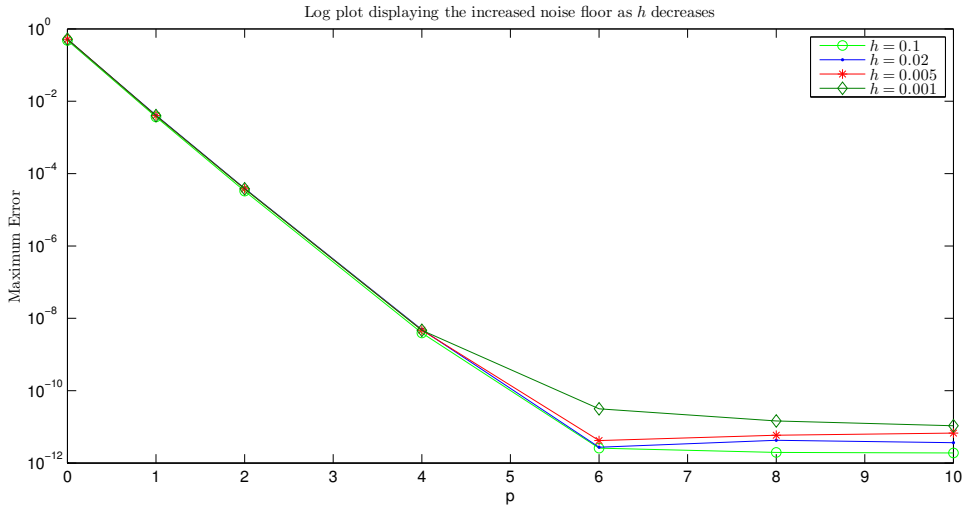

FIGURE 13. The increased noise floor for smaller values of Δt

6. INVERSE PROBLEM

One may use an inverse problem to determine the correct parameters of τ for a two pole Debye model with uniform distributions. Borrowing from their work the procedure is as follows. We begin by defining τ_m to be distributed as,

$$\tau_m \sim \mathcal{U}\left[a_m\overline{\tau}_m, (a_m + b_m)\,\overline{\tau}_m\right] \tag{54}$$

where a_m and b_m are distribution parameters of τ for which we are concerned. We let q be the set of all parameters in the representation of the distribution. This definition is for a uniform distribution, however, any other distribution could be used in its place. Next we define the stochastic complex permittivity as a function of ω, the angular frequency,

$$\varepsilon(\omega) = \varepsilon_\infty + \sum_m \frac{\varepsilon_{d,m}}{1 + \mathrm{i}\omega\tau_m} \tag{55}$$

The expected value of each pole can be found by integrating with respect to the density function of the distribution being used,

$$\mathbb{E}\left[\varepsilon_m(\omega)\right] = \int_{a_m}^{a_m+b_m} \frac{\varepsilon_{d,m}}{1 + \mathrm{i}\omega\tau_m} f(\tau_m)\, d\tau \tag{56}$$

For a uniform distribution this becomes,

$$\mathbb{E}\left[\varepsilon_m(\omega)\right] = \frac{1}{b_m}\left[\int_{a_m\overline{\tau}_m}^{(a_m+b_m)\overline{\tau}_m} \frac{\varepsilon_{d,m}}{1-\omega^2\tau^2} d\tau + \mathrm{i}\int_{a_m\overline{\tau}_m}^{(a_m+b_m)\overline{\tau}} \frac{-\varepsilon_{d,m}\omega\tau}{1-\omega^2\tau^2} d\tau\right] \tag{57}$$

$$= \frac{1}{b_m}\frac{\varepsilon_{d,m}}{\omega}\left[\arctan(\omega\tau) - \frac{\mathrm{i}}{2}\ln\left(1 + (\omega\tau)^2\right)\right]_{a_m\overline{\tau}_m}^{(a_m+b_m)\overline{\tau}_m} \tag{58}$$

While this integral (57) can be evaluated analytically for the uniform distribution, this is not necessarily the case for all distributions. When it may not be exactly evaluated, numerical integration

will suffice. We can evaluate the accuracy of the parameters by evaluating $\varepsilon(\omega)$ across a vector of important frequencies and then subtracting from a target solution, be it real world data or another model such as the Cole-Cole. This subtraction produces a vector of residuals, $R(\omega)$, which can be used to determine the cost, J, defined as,

$$J(\omega) := R^T R \tag{59}$$

Minimizing this cost function will produce the most accurate approximation to the real distribution of τ for each pole.

7. Conclusion

We have shown we can improve the traditional Debye model by replacing the average relaxation time $\bar{\tau}$ with a distribution of relaxation times. The method of Generalized Polynomial Chaos provides us with a convenient means of representing the stochastic polarization, $\mathcal{P}$ as a linear combination of orthogonal polynomials. By projecting into finite random space, we are able to replace a stochastic ordinary differential equation with a system of deterministic ODEs. Combining these with Maxwell's and Faraday's Law and noting that the electric field E depends only on the macroscopic polarization $\mathbb{E}(P) \approx \alpha_0$, we obtain the polynomial chaos model (24) for an electromagnetic field propagating through a dispersive dielectric media.

This model lends itself naturally to discretization using the Yee-Scheme with an additional central difference approximation for the polynomial chaos system. From the discretized equations we are able to obtain a series of sequential update equations (37). These can then be used in performing a MATLAB simulation.

We have proved that this method is stable for Legendre polynomials with $p = 1$ if $m \geq 0$, $\nu \leq 1$, and $\varepsilon_s \geq \varepsilon_\infty$. This method can be extended to other types of orthogonal polynomials and for larger values of p. As a future endevor we would like to establish this result for Jacobi polynomials and obtain a beta distribution of relaxation times that more accurately fits our data. Also of interest is being able to generalize our result for any value of p. In the meantime we have numerically verified the stability of Jacobi and Legendre polynomials for various spatial and temporal resolutions and values of p up to 5. In practice, we do not gain accuracy above $p = 6$ due to current limitations on computational precision, and a value of $p = 2$ or $p = 3$ will probably suffice.

References

[1] HT Banks, VA Bokil, and NL Gibson. Analysis of stability and dispersion in a finite element method for Debye and Lorentz dispersive media. *Numerical Methods for Partial Differential Equations*, 25(4), 2009.

[2] H.T. Banks and N.L. Gibson. Electromagnetic inverse problems involving distributions of dielectric mechanisms and parameters. *Quarterly of Applied Mathematics*, 64(4):749–795, 2006.

[3] K. Barrese and N. Chugh. Approximating dispersive mechanisms using the debye model with distributed dielectric parameters, 2008.

[4] CJF Böttcher, OC Van Belle, P. Bordewijk, A. Rip, and D.D. Yue. Theory of electric polarization. *Journal of The Electrochemical Society*, 121:211C, 1974.

[5] K.S. Cole and R.H. Cole. Dispersion and absorption in dielectrics I. Alternating current characteristics. *The Journal of Chemical Physics*, 9:341, 1941.

[6] Bert J. Debusschere, Habib N. Najm, Philippe P. Pébay, Omar M. Knio, Roger G. Ghanem, and Olivier P. Le Maître. Numerical challenges in the use of polynomial chaos representations for stochastic processes. *SIAM Journal on Scientific Computing*, 26(2):698–719, 2004.

[7] P. Debye. *Polar Molecules*. Dover, 1929.

[8] R.S. Edwards, A.C. Marvin, and S.J. Porter. Uncertainty Analyses in the Finite-Difference Time-Domain Method. *IEEE Transactions on Electromagnetic Compatibility*, 52(1):155–163, 2010.
[9] Kira Heater. The fdtd method: Computation and analysis. Master's thesis, University of Montana, 2005.
[10] B.H. Jung and T.K. Sarkar. Solving time domain Helmholtz wave equation with MOD-FDM. *Progress In Electromagnetics Research*, 79:339–352, 2008.
[11] D. Lucor, C.H. Su, and GE Karniadakis. Generalized polynomial chaos and random oscillators. *International Journal for Numerical Methods in Engineering*, 60(3), 2004.
[12] A. Pereda, L.A. Vielva, A. Vegas, and A. Prieto. Analyzing the stability of the fdtd technique by combining the von neumann method with the routh-hurwitz criterion. *Microwave Theory and Techniques, IEEE Transactions on*, 49(2):377 –381, feb 2001.
[13] P.G. Petropoulos. Stability and phase error analysis of FD-TD in dispersive dielectrics. *IEEE transactions on antennas and propagation*, 42(1):62–69, 1994.
[14] John C. Strikwerda. *Finite difference schemes and partial differential equations*. SIAM, 2004.
[15] Gábor Szegö. *Orthogonal Polynomials*. American Mathematical Society, 1975.
[16] D. Webbe and M. Milne. Simulating polydisperse materials with distributions of the debye model, 2009.
[17] D. Xiu and G.E. Karniadakis. The Wiener–Askey Polynomial Chaos for Stochastic Differential Equations. *SIAM Journal on Scientific Computing*, 24(2):619–644, 2003.
[18] Dongbin Xiu. *Numerical Methods for Stochastic Computations*. Princeton University Press, 2010.
[19] Kane Yee. Numerical solution of initial boundary value problems involving maxwell's equations in isotropic media. *Antennas and Propagation, IEEE Transactions on*, 14(3):302 –307, may 1966.

Appendix A. Variables and Constants

a_n, b_n, c_n - Coefficients from the recurrence relation for orthogonal polynomials
c - speed of light(free space) $c = \frac{1}{\sqrt{\mu_0 \varepsilon_0}}$; also $c_\infty = \frac{c}{\sqrt{\varepsilon_\infty}}$
e - the number e
$\vec{f} = [\tilde{\varepsilon}_d E, 0, \cdots, 0]^T$; the vector found in the system $A\vec{\alpha}(t) + \vec{\alpha}(t) = \vec{f}$
$\tilde{f}^n$, found in modified α system (23)
$h = \frac{\Delta t}{\tau}$
i -index for orthogonal polynomials
$\mathrm{i} = \sqrt{-1}$
j - spatial step, also used as an index for our polynomials in section 2
$k = \frac{\omega}{c}$ - the wave number
m - midpoint between a and b in the distribution of the relaxation time τ n -time step
p - number of polynomials used in the polynomial chaos expansion
q_k - coefficients of the characteristic polynomial (as a function of ζ)
$\hat{q}_k$ - coefficients of the transformed characteristic polynomial (as a function of z)
r - distance from midpoint to the edge of the distribution of τ
t - time
x, y, z - spatial dimensions

A - matrix from the polynomial chaos system, $\mathrm{A}\vec{\alpha}(t) + \vec{\alpha}(t) = \vec{f}$. Note $\mathrm{A} = r\mathrm{M} + m\mathrm{I}$.
$\tilde{\mathrm{A}}$ - modified form of A; add κ to (1,1) entry
B - Magnetic flux density (vector)
D - Electric flux density (vector)
E - Electric Field vector, $E := E_x$
H - Magnetic Field vector, $H := H_y$

I - Identity Matrix
$\mathbf{J}$ -conduction current density, $J := J_x$
$\mathbf{J_s}$ - source current density
M - matrix of recurrence relation coefficients obtained in polynomial chaos expansion
$\mathbf{M}$ -magnetization
$\mathbf{P}$ -macroscopic polarization
$\mathcal{P}$ - stochastic polarization
S - system obtained during stability analysis
W - weighting function

α_i - coefficients from the polynomial chaos expansion of the stochastic polarization (18)
α and β - Beta distribution parameters
δ_{ij} -Kronecker delta function
ε_0 - permittivity of free space
ε_s -static permitttivity
ε_∞ -relative permittivity or infinite frequency permittivity, $\tilde{\varepsilon}_\infty = \varepsilon_0\varepsilon_\infty$
$\varepsilon_d = \varepsilon_s - \varepsilon_\infty$; $\tilde{\varepsilon}_d = \varepsilon_0(\varepsilon_s - \varepsilon_\infty)$
$\varepsilon_q = \frac{\varepsilon_s}{\varepsilon_\infty}$
ζ - complex time eigenvalue
$\theta = 2\varepsilon_\infty + \sigma\Delta t$
$\theta^* = 2\varepsilon_\infty - \sigma\Delta t$
κ - a simplification equal to $\frac{\tilde{\varepsilon}_d \Delta t}{\theta}$
λ - wavelength
μ - magnetic permeability
μ_0 - magnetic permeability of free space
$\nu = \frac{c_\infty \Delta t}{\Delta z}$, courant number
ξ - our random variable
π - for the number pi
ρ - in section 1.1 the density of free electric charges unaccounted for in the electric polarization; elsewhere $\rho = \nu \sin(\frac{k\Delta z}{2})$
σ - electric conductivity
τ - relaxation time
ϕ_i - the ith orthogonal polynomial
ω - angular frequency

Mathematical Operators Σ, Δ
B - Beta Function
Γ - Gamma Function
Ω - the domain of the distribution

CHAPMAN UNIVERSITY
E-mail address: bela100@chapman.edu

OREGON STATE UNIVERSITY
E-mail address: hortsche@gmail.com